The Bethe−Salpeter Equation Formalism: From Physics to Chemistry

Xavier Blase,* Ivan Duchemin, Denis Jacquemin, and Pierre-François Loos*

ACCESS | Metrics & More | Article Recommendations

ABSTRACT: The Bethe−Salpeter equation (BSE) formalism is steadily asserting itself as a new efficient and accurate tool in the ensemble of computational methods available to chemists in order to predict optical excitations in molecular systems. In particular, the combination of the so-called *GW* approximation, giving access to reliable ionization energies and electron affinities, and the BSE formalism, able to model UV/vis spectra, has shown to provide accurate singlet excitation energies with a typical error of 0.1−0.3 eV. With a similar computational cost as time-dependent density-functional theory (TD-DFT), BSE is able to provide an accuracy on par with the most accurate global and range-separated hybrid functionals without the unsettling choice of the exchange−correlation functional, resolving further known issues (e.g., charge-transfer excitations). In this Perspective, we provide a historical overview of BSE, with a particular focus on its condensed-matter roots. We also propose a critical review of its strengths and weaknesses in different chemical situations.
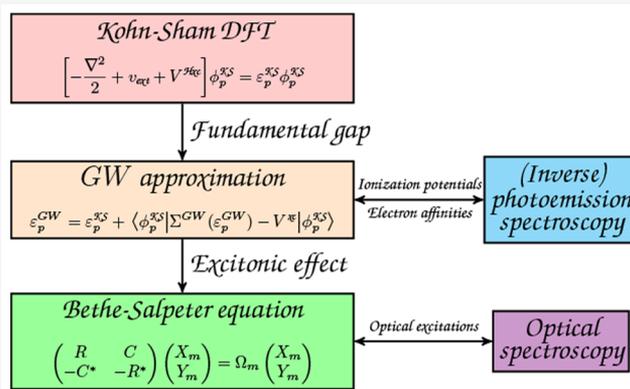
In its press release announcing the awarding of the 2013 Nobel prize in Chemistry to Karplus, Levitt, and Warshel, the Royal Swedish Academy of Sciences concluded by stating "Today the computer is just as important a tool for chemists as the test tube. Simulations are so realistic that they predict the outcome of traditional experiments."[1] Martin Karplus's Nobel lecture moderated this statement, introducing his presentation by a 1929 quote from Dirac emphasizing that laws of quantum mechanics are "much too complicated to be soluble", urging scientists to develop "approximate practical methods". This is where the electronic structure community stands, attempting to develop robust approximations to study with increasing accuracy the properties of ever more complex systems. The study of optical excitations (also known as neutral excitations in condensed-matter systems), from molecules to extended solids, has witnessed the development of a large number of such approximate methods with numerous applications to a large variety of fields, from the prediction of the color of precious metals for jewelry[2] to the understanding, e.g., of the basic principles behind organic photovoltaics, photocatalysis, and DNA damage under irradiation.[3−5] The present Perspective aims at describing the current status and upcoming challenges for the Bethe−Salpeter equation (BSE) formalism[6,7] that, while sharing many features with time-dependent density-functional theory (TD-DFT),[8] including computational scaling with system size, relies on a very different formalism, with specific difficulties but also potential solutions to known TD-DFT issues.[9]

Theory. The BSE formalism[6,7,10−13] belongs to the family of Green's function many-body perturbation theories (MBPT)[14−16] together with, for example, the algebraic-diagrammatic construction (ADC) techniques[17] or the polarization propagator approaches (like SOPPA[18]) in quantum chemistry. While the one-body density stands as the basic variable in density-functional theory (DFT),[19,20] the pillar of Green's function MBPT is the (time-ordered) one-body Green's function

$$G(\boldsymbol{x}t, \boldsymbol{x}'t') = -i\langle N|T[\hat{\psi}(\boldsymbol{x}t)\hat{\psi}^{\dagger}(\boldsymbol{x}'t')]|N\rangle \qquad (1)$$

where $|N\rangle$ is the N-electron ground-state wave function. The operators $\hat{\psi}(\boldsymbol{x}t)$ and $\hat{\psi}^{\dagger}(\boldsymbol{x}'t')$ remove and add an electron (respectively) in space-spin-time positions $(\boldsymbol{x}t)$ and $(\boldsymbol{x}'t')$, while T is the time-ordering operator. For $t > t'$, G provides the amplitude of probability of finding, on top of the ground-state Fermi sea (i.e., higher in energy than the highest-occupied energy level), an electron in $(\boldsymbol{x}t)$ that was previously introduced in $(\boldsymbol{x}'t')$, while for $t < t'$ the propagation of an electron hole (often simply called a hole) is monitored.

This definition indicates that the one-body Green's function is well-suited to obtain "charged excitations", more commonly labeled as electronic energy levels, as obtained, e.g., in direct or inverse photoemission experiments where an electron is ejected or added to the N-electron system. In particular, and as opposed to Kohn−Sham (KS) DFT, the Green's function formalism offers a more rigorous and systematically improvable path for obtaining the ionization potential $I^N = E_0^{N-1} - E_0^N$, the electronic affinity $A^N = E_0^N - E_0^{N+1}$, and the experimental (photoemission) fundamental gap

$$E_g^{\text{fund}} = I^N - A^N \tag{2}$$

of the N-electron system, where E_0^N corresponds to its ground-state energy. Because these energy levels are key input quantities for the subsequent BSE calculation, we start by discussing these in some detail.

Charged Excitations. A central property of the one-body Green's function is that its frequency-dependent (i.e., dynamical) spectral representation has poles at the charged excitation energies (i.e., the ionization potentials and electron affinities) of the system

$$G(\boldsymbol{x}, \boldsymbol{x}'; \omega) = \sum_s \frac{f_s(\boldsymbol{x}) f_s^*(\boldsymbol{x}')}{\omega - \varepsilon_s + i\eta \times \text{sgn}(\varepsilon_s - \mu)} \tag{3}$$

where μ is the chemical potential and η is a positive infinitesimal; $\varepsilon_s = E_s^{N+1} - E_0^N$ for $\varepsilon_s > \mu$, and $\varepsilon_s = E_0^N - E_s^{N-1}$ for $\varepsilon_s < \mu$. Here, E_s^N is the total energy of the sth excited state of the N-electron system. The f_s's are the so-called Lehmann amplitudes that reduce to one-body orbitals in the case of single-determinant many-body wave functions (see below). Unlike KS eigenvalues, the poles of the Green's function $\{\varepsilon_s\}$ are proper addition/removal energies of the N-electron system, leading to well-defined ionization potentials and electronic affinities. In contrast to standard ΔSCF techniques, the knowledge of G provides the full ionization spectrum, as measured by direct and inverse photoemission spectroscopy, not only that associated with frontier orbitals.

Using the equation-of-motion formalism for the creation−destruction operators, it can be shown formally that G verifies

$$\left[\frac{\partial}{\partial t_1} - h(\boldsymbol{r}_1) \right] G(1, 2) - \int d3 \Sigma(1, 3) G(3, 2) = \delta(1, 2) \tag{4}$$

where we introduce the composite index, e.g., $1 \equiv (\boldsymbol{x}_1 t_1)$. Here, δ is Dirac's delta function, h the one-body Hartree Hamiltonian, and Σ the so-called exchange−correlation (xc) self-energy operator. Using the spectral representation of G (see eq 3), dropping spin variables for simplicity, one gets the familiar eigenvalue equation, i.e.,

$$h(\boldsymbol{r}) f_s(\boldsymbol{r}) + \int d\boldsymbol{r}' \Sigma(\boldsymbol{r}, \boldsymbol{r}'; \varepsilon_s) f_s(\boldsymbol{r}') = \varepsilon_s f_s(\boldsymbol{r}) \tag{5}$$

which formally resembles the KS equation[20] with the difference that the self-energy Σ is nonlocal, energy-dependent, and nonhermitian. The knowledge of Σ allows us to access the true addition/removal energies, namely, the entire spectrum of occupied and virtual electronic energy levels, at the cost of solving a generalized one-body eigenvalue equation.

The GW Self-Energy. While the equations reported above are formally exact, it remains to provide an expression for the xc self-energy operator Σ. This is where Green's function practical theories differ. Developed by Lars Hedin in 1965 with

application to the interacting homogeneous electron gas,[14] the GW approximation[15,21] follows the path of linear response by considering the variation of G with respect to an external perturbation (see Figure 1). The resulting equation, when
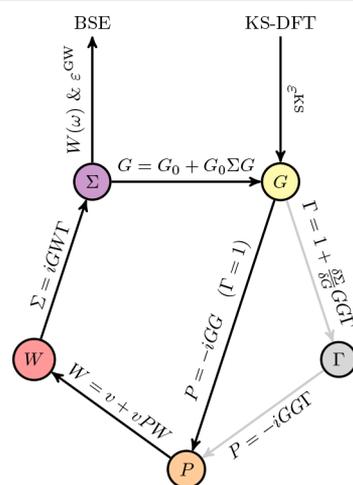
Figure 1. Hedin's pentagon connects the Green's function G, its noninteracting analogue G_0, the irreducible vertex function Γ, the irreducible polarizability P, the dynamically screened Coulomb potential W, and the self-energy Σ through a set of five integro-differential equations known as Hedin's equations.[14] The path made of black arrows shows the GW process which bypasses the computation of Γ (gray arrows). As input, one must provide KS (or HF) orbitals and their corresponding energies. Depending on the level of self-consistency in the GW calculation, only the orbital energies or both the orbitals and their energies are corrected. As output, GW provides corrected quantities, i.e., quasiparticle energies and W, which can then be used to compute the BSE optical excitations of the system of interest.

compared with the equation for the time-evolution of G (see eq 4), leads to a formal expression for the self-energy

$$\Sigma(1, 2) = i \int d34\, G(1, 4) W(3, 1^+) \Gamma(42, 3) \tag{6}$$

where W is the dynamically screened Coulomb potential and Γ is the so-called "vertex" function. The notation 1^+ means that the time t_1 is taken at $t_1^+ = t_1 + 0^+$ for the sake of causality, where 0^+ is a positive infinitesimal. The neglect of the vertex, i.e., $\Gamma(42, 3) = \delta(23)\delta(24)$, leads to the so-called GW approximation of the self-energy

$$\Sigma^{GW}(1, 2) = i G(1, 2) W(2, 1^+) \tag{7}$$

that can be regarded as the lowest-order perturbation in terms of the screened Coulomb potential W with

$$W(1, 2) = v(1, 2) + \int d34\, v(1, 3) \chi_0(3, 4) W(4, 2) \tag{8a}$$

$$\chi_0(1, 2) = -i G(1, 2^+) G(2, 1^+) \tag{8b}$$

where χ_0 is the independent electron susceptibility and v the bare Coulomb potential. Equation 8a can be recast as

$$W(1, 2) = v(1, 2) + \int d34\, v(1, 3) \chi(3, 4) v(4, 2) \tag{9}$$

where χ is the interacting susceptibility. In this latter expression, $(v\chi v)$ represents the field created in (2) by the charge rearrangement of the N-electron system generated by a (unit)

charge added in (1). As such, this term contains the effect of dielectric screening (or polarization in a quantum chemist language). As in a standard ΔSCF calculation, the GW formalism contains the response of the N-electron system to an electron added (removed) to any virtual (occupied) molecular orbital, but without the restriction that only frontier orbitals can be tackled. This explains that the GW one-electron energies are proper addition/removal energies.

In practice, the input G and χ_0 required to initially build Σ^{GW} are chosen as the "best" Green's function and susceptibility that can be easily computed, namely, the KS or Hartree−Fock (HF) ones where the $\{\varepsilon_p, f_p\}$ of eq 3 are taken to be KS (or HF) eigenstates. Taking then $(\Sigma^{GW} - V^{xc})$ as a correction to the KS xc potential V^{xc}, a first-order correction to the input KS energies $\{\varepsilon_p^{KS}\}$ is obtained by solving the so-called quasiparticle equation

$$\omega = \varepsilon_p^{KS} + \langle \phi_p^{KS} | \Sigma^{GW}(\omega) - V^{xc} | \phi_p^{KS} \rangle \tag{10}$$

As a nonlinear equation, the self-consistent quasiparticle eq 10 has various solutions associated with different spectral weights. The existence of a well-defined quasiparticle energy requires a solution with a large spectral weight, i.e., close to unity, a condition not always fulfilled for states far from the fundamental gap.[22]

Such an approach, where input KS energies are corrected to yield better electronic energy levels, is labeled as the single-shot, or perturbative, G_0W_0 technique. This simple scheme was used in the early GW studies of extended semiconductors and insulators,[23−26] and surfaces,[27−29] allowing the dramatic reduction of the errors associated with KS eigenvalues in conjunction with common local or gradient-corrected approximations to the xc potential. In particular, the well-known "band gap" problem,[30,31] namely, the underestimation of the occupied to unoccupied bands energy gap at the KS local-density approximation (LDA) level, was dramatically reduced, bringing the agreement with experiment to within a few tenths of an electronvolt with a computational cost scaling quartically with the system size (see below). A compilation of data for G_0W_0 applied to extended inorganic semiconductors can be found in ref 32.

Although G_0W_0 provides accurate results (at least for weakly/moderately correlated systems), it is strongly starting-point-dependent because of its perturbative nature. For example, the quasiparticle energies, and in particular the HOMO−LUMO gap, depends on the input KS eigenvalues. Tuning the starting point functional or applying a self-consistent GW scheme are two different approaches commonly employed to tackle this problem. We will comment further on this particular point below when addressing the quality of the BSE optical excitations.

> We hope that, by providing a snapshot of the ability of BSE in 2020, the present Perspective will motivate a larger community to participate in the development of this alternative to TD-DFT which, we believe, may become a very valuable computational tool for the physical chemistry community.

Another important feature compared to other perturbative techniques, the GW formalism can tackle finite and periodic systems and does not present any divergence in the limit of zero gap (metallic) systems.[33] However, remaining a low-order perturbative approach starting with a single-determinant mean-field solution, it is not intended to explore strongly correlated systems.[34]

Neutral Excitations. Like TD-DFT, BSE deals with the calculations of optical (or neutral) excitations, as measured by optical (e.g., absorption) spectroscopy. However, while TD-DFT starts with the variation of the charge density $\rho(1)$ with respect to an external local perturbation $U(2)$, the BSE formalism considers a generalized four-point susceptibility, or two-particle correlation function, that monitors the variation of the one-body Green's function $G(1, 1')$ with respect to a nonlocal external perturbation $U(2, 2')$:[7]

$$\chi(1, 2) \overset{DFT}{=} \frac{\partial \rho(1)}{\partial U(2)} \quad \rightarrow \quad L(1, 2; 1', 2') \overset{BSE}{=} \frac{\partial G(1, 1')}{\partial U(2', 2)} \tag{11}$$

The formal relation $\chi(1, 2) = -iL(1, 2; 1^+, 2^+)$ with $\rho(1) = -iG(1, 1^+)$ offers a direct bridge between the TD-DFT and BSE worlds. The equation of motion for G (see eq 4) can be reformulated in the form of a Dyson equation

$$G = G_0 + G_0(v_H + U + \Sigma)G \tag{12}$$

that relates the full (interacting) Green's function, G, to its noninteracting version, G_0, where v_H and U are the Hartree and external potentials, respectively. The derivative with respect to U of this Dyson equation yields the self-consistent Bethe−Salpeter equation

$$L(1, 2; 1', 2') = L_0(1, 2; 1', 2')$$
$$+ \int d3456 L_0(1, 4; 1', 3)\Xi^{BSE}(3, 5; 4, 6)L(6, 2; 5, 2') \tag{13}$$

where $L_0(1, 2; 1', 2') = G(1, 2')G(2, 1')$ is the noninteracting 4-point susceptibility and

$$i\Xi^{BSE}(3, 5; 4, 6) = v(3, 6)\delta(34)\delta(56) + i\frac{\partial\Sigma(3, 4)}{\partial G(6, 5)} \tag{14}$$

is the so-called BSE kernel. This equation can be compared to its TD-DFT analogue

$$\chi(1, 2) = \chi_0(1, 2) + \int d34 \chi_0(1, 3)\Xi^{DFT}(3, 4)\chi(4, 2) \tag{15}$$

where

$$\Xi^{DFT}(3, 4) = v(3, 4) + \frac{\partial V^{xc}(3)}{\partial \rho(4)} \tag{16}$$

is the TD-DFT kernel. Plugging now the GW self-energy (see eq 7), in a scheme that we label BSE@GW, leads to an approximate version of the BSE kernel

$$i\Xi^{BSE}(3, 5; 4, 6) = v(3, 6)\delta(34)\delta(56)$$
$$- W(3^+, 4)\delta(36)\delta(45) \tag{17}$$

where it is customary to neglect the derivative $(\partial W/\partial G)$ that introduces again higher orders in W.[35−37] At that stage, the BSE kernel is fully dynamical, i.e., it explicitly depends on the
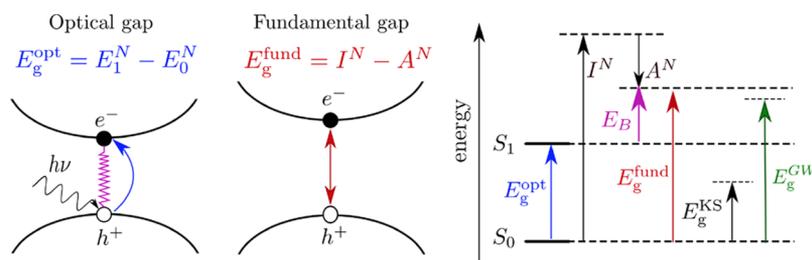
Figure 2. Definition of the optical gap E_g^{opt} and fundamental gap E_g^{fund}. E_B is the electron−hole or excitonic binding energy, while I^N and A^N are the ionization potential and the electron affinity of the N-electron system. E_g^{KS} and E_g^{GW} are the KS and GW HOMO−LUMO gaps. See main text for the definition of the other quantities.

frequency ω. Taking the static limit, i.e., $W(\omega = 0)$, for the screened Coulomb potential, which replaces the static DFT xc kernel, and expressing eq 13 in the standard product space $\{\phi_i(r)\phi_a(r')\}$ [where (i, j) label occupied spatial orbitals and (a, b) label unoccupied spatial orbitals], leads to an eigenvalue problem similar to the so-called Casida equations in TD-DFT:[38]

$$\begin{pmatrix} R & C \\ -C^* & -R^* \end{pmatrix}\begin{pmatrix} X^m \\ Y^m \end{pmatrix} = \Omega_m \begin{pmatrix} X^m \\ Y^m \end{pmatrix} \qquad (18)$$

with electron−hole (eh) eigenstates written as

$$\psi_m^{eh}(r_e, r_h) = \sum_{ia} [X_{ia}^m \phi_i(r_h)\phi_a(r_e) + Y_{ia}^m \phi_i(r_e)\phi_a(r_h)] \qquad (19)$$

where m indexes the electronic excitations. The $\{\phi_{i/a}\}$ are typically the input (KS) eigenstates used to build the GW self-energy. They are here taken to be real in the case of finite-size systems. In the case of a closed-shell singlet ground state, the resonant and coupling parts of the BSE Hamiltonian read

$$R_{ai,bj} = (\varepsilon_a^{GW} - \varepsilon_i^{GW})\delta_{ij}\delta_{ab} + \kappa(ia|jb) - W_{ij,ab} \qquad (20)$$

$$C_{ai,bj} = \kappa(ia|bj) - W_{ib,aj} \qquad (21)$$

with $\kappa = 2$ or 0 if one targets singlet or triplet excited states (respectively), and

$$W_{ij,ab} = \iint dr\,dr'\,\phi_i(r)\phi_j(r)W(r, r'; \omega = 0)\phi_a(r')\phi_b(r') \qquad (22)$$

where we notice that the two occupied (virtual) eigenstates are taken at the same position of space, in contrast with the $(ia|jb)$ bare Coulomb term defined as

$$(ia|jb) = \iint dr\,dr'\,\phi_i(r)\phi_a(r)v(r - r')\phi_j(r')\phi_b(r') \qquad (23)$$

Neglecting the coupling term C between the resonant term R and antiresonant term $-R^*$ in eq 18, leads to the well-known Tamm−Dancoff approximation (TDA).

As compared to TD-DFT, (i) the GW quasiparticle energies $\{\varepsilon_{i/a}^{GW}\}$ replace the KS eigenvalues and (ii) the nonlocal screened Coulomb matrix elements replaces the DFT xc kernel. We emphasize that these equations can be solved at exactly the same cost as the standard TD-DFT equations once the quasiparticle energies and screened Coulomb potential W are inherited from preceding GW calculations. This defines the standard (static) BSE@GW scheme that we discuss in this Perspective, highlighting its pros and cons.

Historical Overview. Originally developed in the framework of nuclear physics,[6] the BSE formalism has emerged in condensed-matter physics around the 1960s at the tight-binding level with

the study of the optical properties of simple semiconductors.[37,39,40] Three decades later, the first *ab initio* implementations, starting with small clusters,[11,41] extended semiconductors, and wide-gap insulators,[12,42,43] paved the way to the popularization in the solid-state physics community of the BSE formalism.

Following pioneering applications to periodic polymers and molecules,[44−47] BSE gained much momentum in quantum chemistry[48] with, in particular, several benchmarks[49−56] on large molecular sets performed with the very same parameters (geometries, basis sets, etc.) as the available higher-level reference calculations.[57] Such comparisons were grounded in the development of codes replacing the plane-wave paradigm of solid-state physics by Gaussian basis sets, together with adequate auxiliary bases when resolution-of-the-identity (RI) techniques[58] were used.

An important conclusion drawn from these calculations was that the quality of the BSE excitation energies is strongly correlated to the deviation of the preceding GW HOMO−LUMO gap

$$E_g^{GW} = \varepsilon_{LUMO}^{GW} - \varepsilon_{HOMO}^{GW} \qquad (24)$$

with the experimental (photoemission) fundamental gap defined in eq 2.

Standard G_0W_0 calculations starting with KS eigenstates generated with (semi)local functionals yield much larger HOMO−LUMO gaps than the input KS gap

$$E_g^{KS} = \varepsilon_{LUMO}^{KS} - \varepsilon_{HOMO}^{KS} \qquad (25)$$

but still too small as compared to the experimental value, i.e.

$$E_g^{KS} \ll E_g^{G_0W_0} < E_g^{fund} \qquad (26)$$

Such a residual discrepancy has been attributed by several authors to "overscreening", namely, the effect associated with building the susceptibility χ based on a grossly underestimated (KS) band gap. This leads to a spurious enhancement of the screening or polarization and, consequently, to an underestimated G_0W_0 gap as compared to the (exact) fundamental gap. More prosaically, the G_0W_0 approach is constructed as a first-order perturbation theory, so by correcting a very "bad" zeroth-order KS system one cannot expect to obtain an accurate corrected gap. Such an underestimation of the fundamental gap leads to a similar underestimation of the optical gap E_g^{opt}, i.e., the lowest optical excitation energy:

$$E_g^{opt} = E_1^N - E_0^N = E_g^{fund} + E_B \qquad (27)$$

where E_B accounts for the excitonic effect, that is, the stabilization induced by the attraction of the excited electron and its hole left behind (see Figure 2).

Such a residual gap problem can be significantly improved by adopting xc functionals with a tuned amount of exact exchange[59,60] that yield a much improved KS gap as a starting point for the GW correction.[56,61−63] Alternatively, self-consistent approaches such as eigenvalue self-consistent (evGW)[24] or quasiparticle self-consistent (qsGW)[64] schemes, where corrected eigenvalues, and possibly orbitals, are reinjected in the construction of G and W, have been shown to lead to a significant improvement of the quasiparticle energies in the case of molecular systems, with the advantage of significantly removing the dependence on the starting point functional.[62,65−69] As a result, BSE singlet excitation energies starting from such improved quasiparticle energies were found to be in much better agreement with reference calculations. For sake of illustration, an average error of 0.2 eV was found for the well-known Thiel set[57] gathering ca. 200 representative singlet excitations from a large variety of representative molecules.[50,51,55,56] This is equivalent to the best TD-DFT results obtained by scanning a large variety of hybrid functionals with various amounts of exact exchange.

Charge-Transfer Excited States. A very remarkable success of the BSE formalism lies in the description of charge-transfer

> A very remarkable success of the BSE formalism lies in the description of charge-transfer (CT) excitations, a notoriously difficult problem for TD-DFT adopting standard (semi)local functionals.

(CT) excitations, a notoriously difficult problem for TD-DFT adopting standard (semi)local functionals.[70] Similar difficulties emerge in solid-state physics for semiconductors where extended Wannier excitons, characterized by weakly overlapping electrons and holes (Figure 3), cause a dramatic deficit of spectral weight at low energy.[71] These difficulties can be ascribed to the lack of long-range electron−hole interaction with local xc functionals. It can be cured through an exact exchange contribution, a solution that explains the success of (optimally tuned) range-separated hybrids for the description of CT excitations.[59,60] The analysis of the screened Coulomb potential matrix elements in the BSE kernel (see eq 17) reveals that such long-range (nonlocal) electron−hole interactions are properly described, including in environments (solvents, molecular solid, etc.) where the screening reduces the long-range electron−hole interactions. The success of the BSE formalism to treat CT excitations has been demonstrated in several studies,[66,72−79] opening the way to the modeling of key applications such as doping,[80] photovoltaics, or photocatalysis in organic systems.

Combining BSE with PCM and QM/MM Models. The ability to account for the effect on the excitation energies of an electrostatic and dielectric environment (an electrode, a solvent, a molecular interface, *etc.*) is an important step toward the description of realistic systems. Pioneering BSE studies demonstrated, for example, the large renormalization of charged and neutral excitations in molecular systems and nanotubes close to a metallic electrode or in bundles.[74,81,82] Recent attempts to merge the GW and BSE formalisms with model
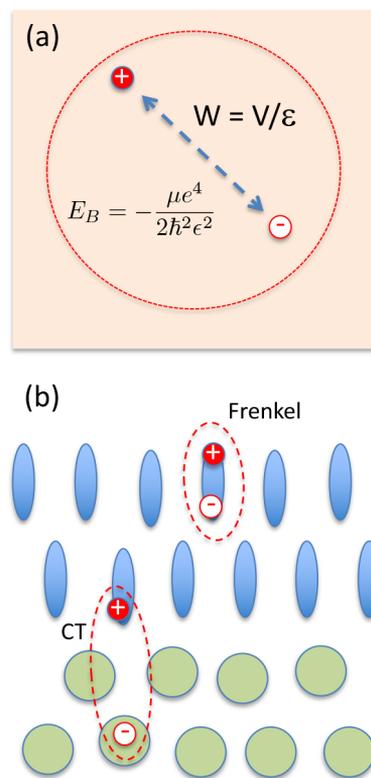
Figure 3. Symbolic representation of (a) extended Wannier exciton with large electron−hole average distance, and (b) Frenkel (local) and charge-transfer (CT) excitations at a donor−acceptor interface. Wannier and CT excitations require long-range electron−hole interaction accounting for the host dielectric constant. In the case of Wannier excitons, the binding energy E_B can be well approximated by the standard hydrogenoid model where μ is the effective mass and ϵ is the dielectric constant.

polarizable environments at the PCM or QM/MM levels[83−89] paved the way not only to interesting applications but also to a better understanding of the merits of these approaches relying on the use of the screened Coulomb potential designed to capture polarization effects at all spatial ranges. As a matter of fact, dressing the bare Coulomb potential with the reaction field matrix $[v(r, r') \rightarrow v(r, r') + v^{\text{reac}}(r, r'; \omega)]$ in the relation between the screened Coulomb potential W and the independent-electron susceptibility (see eq 8a) allows us to perform GW and BSE calculations in a polarizable environment at the same computational cost as the corresponding gas-phase calculation. The reaction field operator $v^{\text{reac}}(r, r'; \omega)$ describes the potential generated in r' by the charge rearrangements in the polarizable environment induced by a source charge located in r, where r and r' lie in the quantum mechanical subsystem of interest. The reaction field is dynamical because the dielectric properties of the environment, such as the macroscopic dielectric constant $\epsilon_M(\omega)$, are in principle frequency dependent. Once the reaction field matrix is known, with typically $\mathcal{O}[N_{\text{orb}}N_{\text{MM}}^2]$ operations (where N_{orb} is the number of orbitals and N_{MM} the number of polarizable atoms in the environment), the full spectrum of GW quasiparticle energies and BSE neutral excitations can be renormalized by the effect of the environment.

A remarkable property[87] of the scheme described above, which combines the BSE formalism with a polarizable environment, is that the renormalization of the electron−electron and electron−hole interactions by the reaction field

captures both linear-response and state-specific contributions[90] to the solvatochromic shift of the optical lines, allowing treatment on the same footing for local (Frenkel) and CT excitations. This is an important advantage as compared to, e.g., TD-DFT where linear-response and state-specific effects have to be explored with different formalisms.

To date, environmental effects on fast electronic excitations are included only by considering the low-frequency optical response of the polarizable medium (e.g., considering the $\epsilon_\infty \approx$ 1.78 macroscopic dielectric constant of water in the optical range), neglecting the frequency dependence of the dielectric constant in the optical range. Generalization to fully frequency-dependent polarizable properties of the environment would allow exploring systems where the relative dynamics of the solute and the solvent are not decoupled, i.e., situations where neither the adiabatic nor the antiadiabatic limits are expected to be valid (for a recent discussion, see ref 91).

We now leave the description of successes to discuss difficulties and future directions of developments and improvements.

The Computational Challenge. As emphasized above, the BSE eigenvalue equation in the single-excitation space (see eq 18) is formally equivalent to that of TD-DFT or TD-HF.[92] Searching iteratively for the lowest eigenstates exhibits the same $O[N_{orb}^4]$ matrix–vector multiplication computational cost within BSE and TD-DFT. Concerning the construction of the BSE Hamiltonian, it is no more expensive than building its TD-DFT analogue with hybrid functionals, reducing again to $O[N_{orb}^4]$ operations with standard RI techniques. Explicit calculation of the full BSE Hamiltonian in transition space can be further avoided using density matrix perturbation theory,[72,93] not reducing though the $O[N_{orb}^4]$ scaling, but sacrificing further the knowledge of the eigenvectors. Exploiting further the locality of the atomic orbital basis, the BSE absorption spectrum can be obtained with $O[N_{orb}^3]$ operations using such iterative techniques.[94] With the same restriction on the eigenvectors, a time-propagation approach, similar to that implemented for TD-DFT,[95] combined with stochastic techniques to reduce the cost of building the BSE Hamiltonian matrix elements, allows quadratic scaling with systems size.[96]

In practice, the main bottleneck for standard BSE calculations as compared to TD-DFT resides in the preceding GW calculation that scales as $O[N_{orb}^4]$ with system size using plane-wave basis sets or RI techniques, but with a rather large prefactor. The field of low-scaling GW calculations is however witnessing significant advances. While the sparsity of, for example, the overlap matrix in the atomic orbital basis allows reducing the scaling in the large size limit,[97,98] efficient real-space grids and time techniques are blooming,[99,100] borrowing in particular the well-known Laplace transform approach used in quantum chemistry.[101] Together with a stochastic sampling of virtual states, this family of techniques allow setting up linear scaling GW calculations.[102] The separability of occupied and virtual states summations lying at the heart of these approaches are now spreading fast in quantum chemistry within the interpolative separable density fitting (ISDF) approach applied to the calculation, with cubic scaling, of the susceptibility needed in random-phase approximation (RPA) and GW calculations.[103–105] These ongoing developments pave the way to applying the GW@BSE formalism to systems containing several hundred atoms on standard laboratory clusters.

> Ongoing developments pave the way to applying the GW@BSE formalism to systems containing several hundred atoms on standard laboratory clusters.

The Triplet Instability Challenge. The analysis of the singlet–triplet splitting is central to numerous applications such as singlet fission or thermally activated delayed fluorescence (TADF). From a more theoretical point of view, triplet instabilities that often plague the applicability of TD-DFT are intimately linked to the stability analysis of restricted closed-shell solutions at the HF[106] and KS[107] levels. While TD-DFT with range-separated hybrids can benefit from tuning the range-separation parameter(s) as a mean to act on the triplet instability,[108] BSE calculations do not offer this pragmatic way out because the screened Coulomb potential that builds the kernel does not contain any parameter to tune.

Benchmark calculations[109,110] clearly concluded that triplets are notably too low in energy within BSE and that the use of the TDA was able to partly reduce this error. However, as it stands, the BSE accuracy for triplets remains rather unsatisfactory for reliable applications. An alternative cure was offered by hybridizing TD-DFT and BSE, that is, by adding to the BSE kernel the correlation part of the underlying DFT functional used to build the susceptibility and resulting screened Coulomb potential W.[111]

The Challenge of the Ground-State Energy. In contrast to TD-DFT which relies on KS-DFT as its ground-state analogue, the ground-state BSE energy is not a well-defined quantity, and no clear consensus has been found regarding its formal definition. Consequently, the BSE ground-state formalism remains in its infancy with very few available studies for atomic and molecular systems.[88,112–115]

A promising route, which closely follows RPA-type formalisms,[116] is to calculate the ground-state BSE energy within the adiabatic-connection fluctuation–dissipation theorem (ACFDT) framework.[117] As a result of comparisons with both similar and state-of-art computational approaches, it was recently shown that the ACFDT@BSE@GW approach yields extremely accurate PES around equilibrium and can even compete with high-order coupled cluster methods in terms of absolute ground-state energies and equilibrium distances.[115] However, their accuracy near the dissociation limit remains an open question.[112,113,118–120] Indeed, in the largest available benchmark study[113] encompassing the total energies of the atoms H–Ne, the atomization energies of the 26 small molecules forming the HEAT test set, and the bond lengths and harmonic vibrational frequencies of 3d transition-metal monoxides, the BSE correlation energy, as evaluated within the ACFDT framework,[117] was mostly discarded from the set of tested techniques because of instabilities (negative frequency modes in the BSE polarization propagator) and replaced by an approximate (RPAsX) approach where the screened-Coulomb potential matrix elements was removed from the resonant electron–hole contribution.[113,121] Moreover, it was also observed in ref 115 that, in some cases, unphysical irregularities on the ground-state PES appear because of the appearance of discontinuities as a function of the bond length for some of the GW quasiparticle energies. Such an unphysical behavior stems from defining the quasiparticle energy as the solution of the

quasiparticle equation with the largest spectral weight in cases where several solutions can be found (see eq 10). We refer the interested reader to refs 22 and 122−125 for detailed discussions.

The Challenge of Analytic Nuclear Gradients. The features of ground- and excited-state potential energy surfaces (PES) are critical for the faithful description and a deeper understanding of photochemical and photophysical processes.[126] For example, chemoluminescence and fluorescence are associated with geometric relaxation of excited states, and structural changes upon electronic excitation.[127] Reliable predictions of these mechanisms, which have attracted much experimental and theoretical interest lately, require exploring the ground- and excited-state PES. From a theoretical point of view, the accurate prediction of excited electronic states remains a challenge,[128] especially for large systems where state-of-the-art computational techniques (such as multiconfigurational methods[129]) cannot be afforded. For the last two decades, TD-DFT has been the go-to method to compute absorption and emission spectra in large molecular systems.

In TD-DFT, the PES for the excited states can be easily and efficiently obtained as a function of the molecular geometry by simply adding the ground-state DFT energy to the excitation energy of the selected state. One of the strongest assets of TD-DFT is the availability of first- and second-order analytic nuclear gradients (i.e., the first- and second-order derivatives of the excited-state energy with respect to atomic displacements), which enables the exploration of excited-state PES.[130]

A significant limitation of the BSE formalism, as compared to TD-DFT, lies in the lack of analytic nuclear gradients for both the ground and excited states, preventing efficient studies of many key excited-state processes. While calculations of the GW quasiparticle energy ionic gradients is becoming increasingly popular,[131−135] only one pioneering study of the excited-state BSE gradients has been published to date.[136] In this seminal work devoted to small molecules (CO and NH_3), only the BSE excitation energy gradients were calculated, with the approximation that the gradient of the screened Coulomb potential can be neglected, computing further the KS-LDA forces as its ground-state contribution.

Beyond the Static Approximation. Going beyond the static approximation is a difficult challenge which has been, nonetheless, embraced by several groups.[7,137−145] As mentioned earlier in this Perspective, most BSE calculations are performed within the so-called static approximation, which substitutes the dynamically screened (i.e., frequency-dependent) Coulomb potential $W(\omega)$ by its static limit $W(\omega = 0)$ (see eq 22). It is important to mention that diagonalizing the BSE Hamiltonian in the static approximation corresponds to solving a *linear* eigenvalue problem in the space of single excitations, while it is, in its dynamical form, a nonlinear eigenvalue problem (in the same space) which is much harder to solve from a numerical point of view. In complete analogy with the ubiquitous adiabatic approximation in TD-DFT, one key consequence of the static approximation is that double (and higher) excitations are completely absent from the BSE optical spectrum, which obviously hampers the applicability of BSE as double excitations may play, indirectly, a key role in photochemistry mechanisms. Higher excitations would be explicitly present in the BSE Hamiltonian by "unfolding" the dynamical BSE kernel, and one would recover a linear eigenvalue problem with, nonetheless, a much larger dimension. Corrections to take into account the dynamical nature of the screening may or may not recover these

multiple excitations. However, dynamical corrections permit, in any case, to recover, for transitions with a dominant single-excitation character, additional relaxation effects coming from higher excitations.

From a more practical point of view, dynamical effects have been found to affect the positions and widths of core-exciton resonances in semiconductors,[36,37] rare gas solids, and transition metals.[146] Using first-order perturbation theory, Rohlfing and co-workers have developed an efficient way of taking into account the dynamical effects via a plasmon-pole approximation combined with the TDA.[137−139,147] With such a scheme, they have been able to compute the excited states of biological chromophores, showing that taking into account the electron−hole dynamical screening is important for an accurate description of the lowest $n \rightarrow \pi^*$ excitations.[138,139,147] Studying PYP, retinal, and GFP chromophore models, Ma et al. found that "the influence of dynamical screening on the excitation energies is about 0.1 eV for the lowest $\pi \rightarrow \pi^*$ transitions, but for the lowest $n \rightarrow \pi^*$ transitions the influence is larger, up to 0.25 eV."[139] Zhang et al. have studied the frequency-dependent second-order BSE kernel, and they have observed an appreciable improvement over configuration interaction with singles (CIS), time-dependent Hartree−Fock (TDHF), and adiabatic TD-DFT results.[143] Rebolini and Toulouse have performed a similar investigation in a range-separated context, and they have reported a modest improvement over its static counterpart.[144] In these two latter studies, they also followed a (nonself-consistent) perturbative approach within the TDA with a renormalization of the first-order perturbative correction.

Conclusion. Although far from being exhaustive, we hope that this Perspective provides a concise and fair assessment of the strengths and weaknesses of the BSE formalism of many-body perturbation theory. To do so, we have briefly reviewed the theoretical aspects behind BSE and its intimate link with the underlying GW calculation that one must perform to compute quasiparticle energies and the dynamically screened Coulomb potential, two of the key input ingredients associated with the BSE formalism. We have then provided a succinct historical overview with a particular focus on its condensed-matter roots and the lessons that the community has learned from several systematic benchmark studies on large molecular systems. Several success stories are then discussed (charge-transfer excited states and combination with reaction field methods), before debating some of the challenges faced by the BSE formalism (computational cost, triplet instabilities, ambiguity in the definition of the ground-state energy, lack of analytic nuclear gradients, and limitations due to the static approximation). We hope that, by providing a snapshot of the ability of BSE in 2020, the present Perspective will motivate a larger community to participate in the development of this alternative to TD-DFT which, we believe, may become a very valuable computational tool for the physical chemistry community.

■ AUTHOR INFORMATION

Corresponding Authors

Xavier Blase − *Université Grenoble Alpes, CNRS, Institut NEEL, F-38042 Grenoble, France;* ⦿ orcid.org/0000-0002-0201-9093; Email: xavier.blase@neel.cnrs.fr

Pierre-François Loos − *Laboratoire de Chimie et Physique Quantiques, Université de Toulouse, CNRS, UPS, Toulouse, France;* ⦿ orcid.org/0000-0003-0598-7425; Email: loos@irsamc.ups-tlse.fr

Authors

Ivan Duchemin − *Université Grenoble Alpes, CEA, IRIG-MEM-L Sim, 38054 Grenoble, France;* ⓘ orcid.org/0000-0003-4713-1174

Denis Jacquemin − *Université de Nantes, CNRS, CEISAM UMR 6230, F-44000 Nantes, France;* ⓘ orcid.org/0000-0002-4217-0708

Complete contact information is available at:
https://pubs.acs.org/10.1021/acs.jpclett.0c01875

Notes

The authors declare no competing financial interest.

Biographies

Xavier Blase holds his Ph.D. in Physics from the University of California at Berkeley. He is presently CNRS Research Director at Institut Néel, Grenoble, France. His research focuses on the electronic and optical properties of systems relevant to condensed matter physics, materials sciences, and physical chemistry, with much emphasis on methodology. He is the coauthor of the FIESTA code (Bull-Fourier prize 2014) that implements the *GW* and Bethe−Salpeter formalisms with Gaussian basis sets. He received the 2008 CNRS silver medal.

Ivan Duchemin holds his Ph.D. from the CEMES in Toulouse, France. He stayed as a postdoctoral fellow at the UC Davis Physics department, California, and the Max Plank Institute for Polymer Research in Mainz, Germany, before joining the French Center for Alternative Energies (CEA), Grenoble, France, as a senior scientist. His research interests focus on methodological and code developments in *ab initio* quantum simulations. He is presently the main developer of the FIESTA code (Bull-Fourier prize 2014).

Denis Jacquemin received his Ph.D. in Chemistry from the University of Namur in 1998, before moving to the University of Florida for his postdoctoral stay. He is currently full Professor at the University of Nantes (France). His research is focused on modeling electronically excited-state processes in organic and inorganic dyes as well as photochromes using a large panel of *ab initio* approaches. His group collaborates with many experimental and theoretical groups. He is the author of more than 500 scientific papers. He has been an ERC grantee (2011−2016) and member of Institut Universitaire de France (2012−2017) and received the WATOC's Dirac Medal (2014).

Pierre-François Loos was born in Nancy, France in 1982. He received his M.S. in Computational and Theoretical Chemistry from the Université Henri Poincaré (Nancy, France) in 2005 and his Ph.D. from the same university in 2008. From 2009 to 2013, he performed postdoctoral research with Peter M. W. Gill at the Australian National University (ANU). From 2013 to 2017, he was a "*Discovery Early Career Researcher Award*" recipient and then a senior lecturer at the ANU. Since 2017, he has held a researcher position from the "*Centre National de la Recherche Scientifique (CNRS)*" at the *Laboratoire de Chimie et Physique Quantiques*" in Toulouse (France), and he was awarded, in 2019, an ERC consolidator grant for the development of new excited-state methodologies.

■ REFERENCES

(1) The Royal Swedish Academy of Sciences. *The Nobel Prize in Chemistry 2013*. Press release, 2013.

(2) Prandini, G.; Rignanese, G.-M.; Marzari, N. Photorealistic Modelling of Metals from First Principles. *npj Comput. Mater.* **2019**, *5*, 129.

(3) Kippelen, B.; Brédas, J.-L. Organic photovoltaics. *Energy Environ. Sci.* **2009**, *2*, 251−261.

(4) Improta, R.; Santoro, F.; Blancafort, L. Quantum Mechanical Studies on the Photophysics and the Photochemistry of Nucleic Acids and Nucleobases. *Chem. Rev.* **2016**, *116*, 3540−3593.

(5) Wu, X.; Choudhuri, I.; Truhlar, D. G. Computational Studies of Photocatalysis with Metal−Organic Frameworks. *Energy Environ. Mater.* **2019**, *2*, 251−263.

(6) Salpeter, E. E.; Bethe, H. A. A Relativistic Equation for Bound-State Problems. *Phys. Rev.* **1951**, *84*, 1232.

(7) Strinati, G. Application of the Green's Functions Method to the Study of the Optical Properties of Semiconductors. *Riv. Nuovo Cimento* **1988**, *11*, 1−86.

(8) Runge, E.; Gross, E. K. U. Density-Functional Theory for Time-Dependent Systems. *Phys. Rev. Lett.* **1984**, *52*, 997−1000.

(9) Blase, X.; Duchemin, I.; Jacquemin, D. The Bethe−Salpeter Equation in Chemistry: Relations with TD-DFT, Applications and Challenges. *Chem. Soc. Rev.* **2018**, *47*, 1022−1043.

(10) Albrecht, S.; Reining, L.; Del Sole, R.; Onida, G. Ab Initio Calculation of Excitonic Effects in the Optical Spectra of Semiconductors. *Phys. Rev. Lett.* **1998**, *80*, 4510−4513.

(11) Rohlfing, M.; Louie, S. G. Electron-Hole Excitations in Semiconductors and Insulators. *Phys. Rev. Lett.* **1998**, *81*, 2312−2315.

(12) Benedict, L. X.; Shirley, E. L.; Bohn, R. B. Optical Absorption of Insulators and the Electron-Hole Interaction: An Ab Initio Calculation. *Phys. Rev. Lett.* **1998**, *80*, 4514−4517.

(13) van der Horst, J.-W.; Bobbert, P. A.; Michels, M. A. J.; Brocks, G.; Kelly, P. J. Ab Initio Calculation of the Electronic and Optical Excitations in Polythiophene: Effects of Intra- and Interchain Screening. *Phys. Rev. Lett.* **1999**, *83*, 4413−4416.

(14) Hedin, L. New Method for Calculating the One-Particle Green's Function with Application to the Electron-Gas Problem. *Phys. Rev.* **1965**, *139*, A796.

(15) Onida, G.; Reining, L.; Rubio, A. Electronic Excitations: Density-Functional Versus Many-Body Green's Function Approaches. *Rev. Mod. Phys.* **2002**, *74*, 601−659.

(16) Martin, R.; Reining, L.; Ceperley, D. *Interacting Electrons: Theory and Computational Approaches*; Cambridge University Press, 2016.

(17) Dreuw, A.; Wormit, M. The Algebraic Diagrammatic Construction Scheme for the Polarization Propagator for the Calculation of Excited States. *Wiley Interdiscip. Rev. Comput. Mol. Sci.* **2015**, *5*, 82−95.

(18) Packer, M. K.; Dalskov, E. K.; Enevoldsen, T.; Jensen, H. J.; Oddershede, J. A New Implementation of the Second-Order Polarization Propagator Approximation (SOPPA): The Excitation Spectra of Benzene and Naphthalene. *J. Chem. Phys.* **1996**, *105*, 5886−5900.

(19) Hohenberg, P.; Kohn, W. Inhomogeneous Electron Gas. *Phys. Rev.* **1964**, *136*, B864−B871.

(20) Kohn, W.; Sham, L. J. Self-Consistent Equations Including Exchange and Correlation Effects. *Phys. Rev.* **1965**, *140*, A1133−A1138.

(21) Golze, D.; Dvorak, M.; Rinke, P. The GW Compendium: A Practical Guide to Theoretical Photoemission Spectroscopy. *Front. Chem.* **2019**, *7*, 377.

(22) Veril, M.; Romaniello, P.; Berger, J. A.; Loos, P. F. Unphysical Discontinuities in GW Methods. *J. Chem. Theory Comput.* **2018**, *14*, 5220.

(23) Strinati, G.; Mattausch, H. J.; Hanke, W. Dynamical Correlation Effects on the Quasiparticle Bloch States of a Covalent Crystal. *Phys. Rev. Lett.* **1980**, *45*, 290−294.

(24) Hybertsen, M. S.; Louie, S. G. Electron Correlation in Semiconductors and Insulators: Band Gaps and Quasiparticle Energies. *Phys. Rev. B: Condens. Matter Mater. Phys.* **1986**, *34*, 5390−5413.

(25) Godby, R. W.; Schlüter, M.; Sham, L. J. Self-Energy Operators and Exchange-Correlation Potentials in Semiconductors. *Phys. Rev. B: Condens. Matter Mater. Phys.* **1988**, *37*, 10159−10175.

(26) von der Linden, W.; Horsch, P. Precise Quasiparticle Energies and Hartree-Fock Bands of Semiconductors and Insulators. *Phys. Rev. B: Condens. Matter Mater. Phys.* **1988**, *37*, 8351−8362.

(27) Northrup, J. E.; Hybertsen, M. S.; Louie, S. G. Many-body Calculation of the Surface-State Energies for Si(111)2 × 1. *Phys. Rev. Lett.* **1991**, *66*, 500−503.

(28) Blase, X.; Zhu, X.; Louie, S. G. Self-Energy Effects on the Surface-State Energies of H-Si(111)1 × 1. *Phys. Rev. B: Condens. Matter Mater. Phys.* **1994**, *49*, 4973−4980.

(29) Rohlfing, M.; Krüger, P.; Pollmann, J. Efficient Scheme for GW Quasiparticle Band-Structure Calculations with Aapplications to Bulk Si and to the Si(001)-(2 × 1) Surface. *Phys. Rev. B: Condens. Matter Mater. Phys.* **1995**, *52*, 1905−1917.

(30) Perdew, J. P.; Levy, M. Physical Content of the Exact Kohn-Sham Orbital Energies: Band Gaps and Derivative Discontinuities. *Phys. Rev. Lett.* **1983**, *51*, 1884−1887.

(31) Sham, L. J.; Schlüter, M. Density-Functional Theory of the Energy Gap. *Phys. Rev. Lett.* **1983**, *51*, 1888−1891.

(32) Shishkin, M.; Kresse, G. Self-Consistent GW Calculations for Semiconductors and Insulators. *Phys. Rev. B: Condens. Matter Mater. Phys.* **2007**, *75*, 235102.

(33) Campillo, I.; Pitarke, J. M.; Rubio, A.; Zarate, E.; Echenique, P. M. Inelastic Lifetimes of Hot Electrons in Real Metals. *Phys. Rev. Lett.* **1999**, *83*, 2230−2233.

(34) Verdozzi, C.; Godby, R. W.; Holloway, S. Evaluation of GW Approximations for the Self-Energy of a Hubbard Cluster. *Phys. Rev. Lett.* **1995**, *74*, 2327−2330.

(35) Hanke, W.; Sham, L. J. Many-Particle Effects in the Optical Spectrum of a Semiconductor. *Phys. Rev. B: Condens. Matter Mater. Phys.* **1980**, *21*, 4656.

(36) Strinati, G. Dynamical Shift and Broadening of Core Excitons in Semiconductors. *Phys. Rev. Lett.* **1982**, *49*, 1519.

(37) Strinati, G. Effects of Dynamical Screening on Resonances at Inner-Shell Thresholds in Semiconductors. *Phys. Rev. B: Condens. Matter Mater. Phys.* **1984**, *29*, 5718.

(38) Casida, M. E. In *Time-Dependent Density Functional Response Theory for Molecules*; Chong, D. P., Ed.; Recent Advances in Density Functional Methods; World Scientific: Singapore, 1995; pp 155−192.

(39) Sham, L. J.; Rice, T. M. Many-Particle Derivation of the Effective-Mass Equation for the Wannier Exciton. *Phys. Rev.* **1966**, *144*, 708−714.

(40) Delerue, C.; Lannoo, M.; Allan, G. Excitonic and Quasiparticle Gaps in Si Nanocrystals. *Phys. Rev. Lett.* **2000**, *84*, 2457−2460.

(41) Onida, G.; Reining, L.; Godby, R. W.; Del Sole, R.; Andreoni, W. Ab Initio Calculations of the Quasiparticle and Absorption Spectra of Clusters: The Sodium Tetramer. *Phys. Rev. Lett.* **1995**, *75*, 818−821.

(42) Albrecht, S.; Onida, G.; Reining, L. Ab initio Calculation of the Quasiparticle Spectrum and Excitonic Effects in Li$_2$O. *Phys. Rev. B: Condens. Matter Mater. Phys.* **1997**, *55*, 10278−10281.

(43) Rohlfing, M.; Louie, S. G. Excitons and Optical Spectrum of the Si(111) − (2 × 1) Surface. *Phys. Rev. Lett.* **1999**, *83*, 856−859.

(44) Rohlfing, M.; Louie, S. G. Optical Excitations in Conjugated Polymers. *Phys. Rev. Lett.* **1999**, *82*, 1959−1962.

(45) van der Horst, J.-W.; Bobbert, P. A.; Michels, M. A. J.; Brocks, G.; Kelly, P. J. Ab Initio Calculation of the Electronic and Optical Excitations in Polythiophene: Effects of Intra- and Interchain Screening. *Phys. Rev. Lett.* **1999**, *83*, 4413−4416.

(46) Puschnig, P.; Ambrosch-Draxl, C. Suppression of Electron-Hole Correlations in 3D Polymer Materials. *Phys. Rev. Lett.* **2002**, *89*, 056405.

(47) Tiago, M. L.; Northrup, J. E.; Louie, S. G. Ab Initio Calculation of the Electronic and Optical Properties of Solid Pentacene. *Phys. Rev. B: Condens. Matter Mater. Phys.* **2003**, *67*, 115212.

(48) See Table 1 of ref 9 for an exhaustive list of applications to molecular systems.

(49) Boulanger, P.; Jacquemin, D.; Duchemin, I.; Blase, X. Fast and Accurate Electronic Excitations in Cyanines with the Many-Body

Bethe−Salpeter Approach. *J. Chem. Theory Comput.* **2014**, *10*, 1212−1218.

(50) Jacquemin, D.; Duchemin, I.; Blase, X. Benchmarking the Bethe−Salpeter Formalism on a Standard Organic Molecular Set. *J. Chem. Theory Comput.* **2015**, *11*, 3290−3304.

(51) Bruneval, F.; Hamed, S. M.; Neaton, J. B. A Systematic Benchmark of the ab initio Bethe-Salpeter Equation Approach for Low-Lying Optical Excitations of Small Organic Molecules. *J. Chem. Phys.* **2015**, *142*, 244101.

(52) Jacquemin, D.; Duchemin, I.; Blase, X. 0−0 Energies Using Hybrid Schemes: Benchmarks of TD-DFT, CIS(D), ADC(2), CC2, and BSE/GW formalisms for 80 Real-Life Compounds. *J. Chem. Theory Comput.* **2015**, *11*, 5340−5359.

(53) Hirose, D.; Noguchi, Y.; Sugino, O. All-Electron GW+Bethe-Salpeter Calculations on Small Molecules. *Phys. Rev. B: Condens. Matter Mater. Phys.* **2015**, *91*, 205111.

(54) Jacquemin, D.; Duchemin, I.; Blase, X. Is the Bethe−Salpeter Formalism Accurate for Excitation Energies? Comparisons with TD-DFT, CASPT2, and EOM-CCSD. *J. Phys. Chem. Lett.* **2017**, *8*, 1524−1529.

(55) Krause, K.; Klopper, W. Implementation of the Bethe-Salpeter equation in the TURBOMOLE program. *J. Comput. Chem.* **2017**, *38*, 383−388.

(56) Gui, X.; Holzer, C.; Klopper, W. Accuracy Assessment of GW Starting Points for Calculating Molecular Excitation Energies Using the Bethe−Salpeter Formalism. *J. Chem. Theory Comput.* **2018**, *14*, 2127−2136.

(57) Schreiber, M.; Silva-Junior, M. R.; Sauer, S. P. A.; Thiel, W. Benchmarks for Electronically Excited States: CASPT2, CC2, CCSD and CC3. *J. Chem. Phys.* **2008**, *128*, 134110.

(58) Ren, X.; Rinke, P.; Blum, V.; Wieferink, J.; Tkatchenko, A.; Sanfilippo, A.; Reuter, K.; Scheffler, M. Resolution-of-identity Approach to Hartree−Fock, Hybrid Fensity Functionals, RPA, MP2 and GW with Numeric Atom-Centered Orbital Basis Functions. *New J. Phys.* **2012**, *14*, 053020.

(59) Stein, T.; Kronik, L.; Baer, R. Reliable Prediction of Charge Transfer Excitations in Molecular Complexes Using Time-Dependent Density Functional Theory. *J. Am. Chem. Soc.* **2009**, *131*, 2818−2820.

(60) Kronik, L.; Stein, T.; Refaely-Abramson, S.; Baer, R. Excitation Gaps of Finite-Sized Systems from Optimally Tuned Range-Separated Hybrid Functionals. *J. Chem. Theory Comput.* **2012**, *8*, 1515−1531.

(61) Bruneval, F.; Marques, M. A. L. Benchmarking the Starting Points of the *GW* Approximation for Molecules. *J. Chem. Theory Comput.* **2013**, *9*, 324−329.

(62) Rangel, T.; Hamed, S. M.; Bruneval, F.; Neaton, J. B. Evaluating the GW Approximation with CCSD(T) for Charged Excitations Across the Oligoacenes. *J. Chem. Theory Comput.* **2016**, *12*, 2834−2842.

(63) Knight, J. W.; Wang, X.; Gallandi, L.; Dolgounitcheva, O.; Ren, X.; Ortiz, J. V.; Rinke, P.; Körzdörfer, T.; Marom, N. Accurate Ionization Potentials and Electron Affinities of Acceptor Molecules III: A Benchmark of *GW* Methods. *J. Chem. Theory Comput.* **2016**, *12*, 615−626.

(64) van Schilfgaarde, M.; Kotani, T.; Faleev, S. Quasiparticle Self-Consistent GW Theory. *Phys. Rev. Lett.* **2006**, *96*, 226402.

(65) Rostgaard, C.; Jacobsen, K. W.; Thygesen, K. S. Fully Self-Consistent GW Calculations for Molecules. *Phys. Rev. B: Condens. Matter Mater. Phys.* **2010**, *81*, 085103.

(66) Blase, X.; Attaccalite, C. Charge-Transfer Excitations in Molecular Donor-Acceptor Complexes within the Many-Body Bethe-Salpeter Approach. *Appl. Phys. Lett.* **2011**, *99*, 171909.

(67) Ke, S.-H. All-Electron G W Methods Implemented in Molecular Orbital Space: Ionization Energy and Electron Affinity of Conjugated Molecules. *Phys. Rev. B: Condens. Matter Mater. Phys.* **2011**, *84*, 205415.

(68) Kaplan, F.; Harding, M. E.; Seiler, C.; Weigend, F.; Evers, F.; van Setten, M. J. Quasi-Particle Self-Consistent *GW* for Molecules. *J. Chem. Theory Comput.* **2016**, *12*, 2528−2541.

(69) Caruso, F.; Dauth, M.; van Setten, M. J.; Rinke, P. Benchmark of GW Approaches for the GW100 Test Set. *J. Chem. Theory Comput.* **2016**, *12*, 5076.

(70) Dreuw, A.; Head-Gordon, M. Failure of Time-Dependent Density Functional Theory for Long-Range Charge-Transfer Excited States: The Zincbacteriochlorin-Bacteriochlorin and Bacteriochlorophyll-Spheroidene Complexes. *J. Am. Chem. Soc.* **2004**, *126*, 4007−4016.

(71) Botti, S.; Sottile, F.; Vast, N.; Olevano, V.; Reining, L.; Weissker, H.-C.; Rubio, A.; Onida, G.; Del Sole, R.; Godby, R. W. Long-Range Contribution to the Exchange-Correlation Kernel of Time-Dependent Density Functional Theory. *Phys. Rev. B: Condens. Matter Mater. Phys.* **2004**, *69*, 155112.

(72) Rocca, D.; Lu, D.; Galli, G. Ab Initio Calculations of Optical Absorption Spectra: Solution of the Bethe−Salpeter Equation Within Density Matrix Perturbation Theory. *J. Chem. Phys.* **2010**, *133*, 164109.

(73) Cudazzo, P.; Attaccalite, C.; Tokatly, I. V.; Rubio, A. Strong Charge-Transfer Excitonic Effects and the Bose−Einstein Exciton Condensate in Graphane. *Phys. Rev. Lett.* **2010**, *104*, 226804.

(74) Garcia-Lastra, J. M.; Thygesen, K. S. Renormalization of Optical Excitations in Molecules Near a Metal Surface. *Phys. Rev. Lett.* **2011**, *106*, 187402.

(75) Baumeier, B.; Andrienko, D.; Rohlfing, M. Frenkel and Charge-Transfer Excitations in Donor−Acceptor Complexes From Many-Body Green's Functions Theory. *J. Chem. Theory Comput.* **2012**, *8*, 2790−2795.

(76) Duchemin, I.; Deutsch, T.; Blase, X. Short-Range to Long-Range Charge-Transfer Excitations in the Zincbacteriochlorin-Bacteriochlorin Complex: A Bethe-Salpeter Study. *Phys. Rev. Lett.* **2012**, *109*, 167801.

(77) Sharifzadeh, S.; Darancet, P.; Kronik, L.; Neaton, J. B. Low-Energy Charge-Transfer Excitons in Organic Solids from First-Principles: The Case of Pentacene. *J. Phys. Chem. Lett.* **2013**, *4*, 2197−2201.

(78) Cudazzo, P.; Gatti, M.; Rubio, A.; Sottile, F. Frenkel versus Charge-Transfer Exciton Dispersion in Molecular Crystals. *Phys. Rev. B: Condens. Matter Mater. Phys.* **2013**, *88*, 195152.

(79) Yin, H.; Ma, Y.; Mu, J.; Liu, C.; Rohlfing, M. Charge-Transfer Excited States in Aqueous DNA: Insights from Many-Body Green's Function Theory. *Phys. Rev. Lett.* **2014**, *112*, 228301.

(80) Li, J.; D'Avino, G.; Pershin, A.; Jacquemin, D.; Duchemin, I.; Beljonne, D.; Blase, X. Correlated electron-hole mechanism for molecular doping in organic semiconductors. *Phys. Rev. Materials* **2017**, *1*, 025602.

(81) Rohlfing, M. Redshift of Excitons in Carbon Nanotubes Caused by the Environment Polarizability. *Phys. Rev. Lett.* **2012**, *108*, 087402.

(82) Spataru, C. D. Electronic and Optical Gap Renormalization in Carbon Nanotubes Near a Metallic Surface. *Phys. Rev. B: Condens. Matter Mater. Phys.* **2013**, *88*, 125412.

(83) Baumeier, B.; Rohlfing, M.; Andrienko, D. Electronic Excitations in Push−Pull Oligomers and Their Complexes with Fullerene from Many-Body Green's Functions Theory with Polarizable Embedding. *J. Chem. Theory Comput.* **2014**, *10*, 3104−3110.

(84) Duchemin, I.; Jacquemin, D.; Blase, X. Combining the GW Formalism with the Polarizable Continuum Model: A State-Specific Non-Equilibrium Approach. *J. Chem. Phys.* **2016**, *144*, 164106.

(85) Li, J.; D'Avino, G.; Duchemin, I.; Beljonne, D.; Blase, X. Combining the Many-Body GW Formalism with Classical Polarizable Models: Insights on the Electronic Structure of Molecular Solids. *J. Phys. Chem. Lett.* **2016**, *7*, 2814−2820.

(86) Varsano, D.; Caprasecca, S.; Coccia, E. Theoretical Description of Protein Field Effects on Electronic Excitations of Biological Chromophores. *J. Phys.: Condens. Matter* **2017**, *29*, 013002.

(87) Duchemin, I.; Guido, C. A.; Jacquemin, D.; Blase, X. The Bethe−Salpeter Formalism with Polarisable Continuum Embedding: Reconciling Linear-Response and State-Specific Features. *Chem. Sci.* **2018**, *9*, 4430−4443.

(88) Li, J.; Drummond, N. D.; Schuck, P.; Olevano, V. Comparing Many-Body Approaches Against the Helium Atom Exact Solution. *SciPost Phys.* **2019**, *6*, 040.

(89) Tirimbò, G.; Sundaram, V.; Çaylak, O.; Scharpach, W.; Sijen, J.; Junghans, C.; Brown, J.; Ruiz, F. Z.; Renaud, N.; Wehner, J.; et al. Excited-state electronic structure of molecules using many-body

Green's functions: Quasiparticles and electron−hole excitations with VOTCA-XTP. *J. Chem. Phys.* **2020**, *152*, 114103.

(90) Cammi, R.; Corni, S.; Mennucci, B.; Tomasi, J. Electronic Excitation Energies of Molecules in Solution: State Specific and Linear Response Methods for Nonequilibrium Continuum Solvation Models. *J. Chem. Phys.* **2005**, *122*, 104513.

(91) Phan Huu, D. K. A.; Dhali, R.; Pieroni, C.; Di Maiolo, F.; Sissa, C.; Terenziani, F.; Painelli, A. Antiadiabatic View of Fast Environmental Effects on Optical Spectra. *Phys. Rev. Lett.* **2020**, *124*, 107401.

(92) Dreuw, A.; Head-Gordon, M. Single-Reference Ab Initio Methods for the Calculation of Excited States of Large Molecules. *Chem. Rev.* **2005**, *105*, 4009−4037.

(93) Nguyen, N. L.; Ma, H.; Govoni, M.; Gygi, F.; Galli, G. Finite-Field Approach to Solving the Bethe-Salpeter Equation. *Phys. Rev. Lett.* **2019**, *122*, 237402.

(94) Ljungberg, M. P.; Koval, P.; Ferrari, F.; Foerster, D.; Sánchez-Portal, D. Cubic-Scaling Iterative Solution of the Bethe-Salpeter Equation for Finite Systems. *Phys. Rev. B: Condens. Matter Mater. Phys.* **2015**, *92*, 075422.

(95) Yabana, K.; Bertsch, G. F. Time-Dependent Local-Density Approximation in Real Time. *Phys. Rev. B: Condens. Matter Mater. Phys.* **1996**, *54*, 4484−4487.

(96) Rabani, E.; Baer, R.; Neuhauser, D. Time-Dependent Stochastic Bethe-Salpeter Approach. *Phys. Rev. B: Condens. Matter Mater. Phys.* **2015**, *91*, 235302.

(97) Foerster, D.; Koval, P.; Sánchez-Portal, D. An O(N3) Implementation of Hedin's GW Approximation for Molecules. *J. Chem. Phys.* **2011**, *135*, 074105.

(98) Wilhelm, J.; Golze, D.; Talirz, L.; Hutter, J.; Pignedoli, C. A. Toward GW Calculations on Thousands of Atoms. *J. Phys. Chem. Lett.* **2018**, *9*, 306−312.

(99) Rojas, H. N.; Godby, R. W.; Needs, R. J. Space-Time Method for Ab Initio Calculations of Self-Energies and Dielectric Response Functions of Solids. *Phys. Rev. Lett.* **1995**, *74*, 1827.

(100) Liu, P.; Kaltak, M.; Klimeš, J. c. v.; Kresse, G. Cubic Scaling *GW*: Towards Fast Quasiparticle Calculations. *Phys. Rev. B: Condens. Matter Mater. Phys.* **2016**, *94*, 165109.

(101) Häser, M.; Almlöf, J. Laplace Transform Techniques in Møller−Plesset Perturbation Theory. *J. Chem. Phys.* **1992**, *96*, 489−494.

(102) Vlček, V.; Rabani, E.; Neuhauser, D.; Baer, R. Stochastic GW Calculations for Molecules. *J. Chem. Theory Comput.* **2017**, *13*, 4997−5003.

(103) Lu, J.; Thicke, K. Cubic Scaling Algorithms for RPA Correlation Using Interpolative Separable Density Fitting. *J. Comput. Phys.* **2017**, *351*, 187−202.

(104) Duchemin, I.; Blase, X. Separable resolution-of-the-identity with all-electron Gaussian bases: Application to cubic-scaling RPA. *J. Chem. Phys.* **2019**, *150*, 174120.

(105) Gao, W.; Chelikowsky, J. R. Accelerating Time-Dependent Density Functional Theory and GW Calculations for Molecules and Nanoclusters with Symmetry Adapted Interpolative Separable Density Fitting. *J. Chem. Theory Comput.* **2020**, *16*, 2216−2223.

(106) Seeger, R.; Pople, J. A. Self-Consistent Molecular Orbital Methods. XVIII. Constraints and Stability in Hartree−Fock Theory. *J. Chem. Phys.* **1977**, *66*, 3045−3050.

(107) Bauernschmitt, R.; Ahlrichs, R. Stability Analysis for Solutions of the Closed Shell Kohn−Sham Equation. *J. Chem. Phys.* **1996**, *104*, 9047−9052.

(108) Sears, J. S.; Koerzdoerfer, T.; Zhang, C.-R.; Brédas, J.-L. Orbital Instabilities and Triplet States fFrom Time-Dependent Density Functional Theory and Long-Range Corrected Functionals. *J. Chem. Phys.* **2011**, *135*, 151103.

(109) Jacquemin, D.; Duchemin, I.; Blondel, A.; Blase, X. Benchmark of Bethe-Salpeter for Triplet Excited-States. *J. Chem. Theory Comput.* **2017**, *13*, 767−783.

(110) Rangel, T.; Hamed, S. M.; Bruneval, F.; Neaton, J. B. An Assessment of Low-Lying Excitation Energies and Triplet Instabilities of Organic Molecules with an *Ab Initio* Bethe-Salpeter Equation

Approach and the Tamm-Dancoff Approximation. *J. Chem. Phys.* **2017**, *146*, 194108.

(111) Holzer, C.; Klopper, W. A Hybrid Bethe−Salpeter/Time-Dependent Density-Functional-Theory Approach for Excitation Energies. *J. Chem. Phys.* **2018**, *149*, 101101.

(112) Olsen, T.; Thygesen, K. S. Static Correlation Beyond the Random Phase Approximation: Dissociating H2 With the Bethe-Salpeter Equation and Time-Dependent GW. *J. Chem. Phys.* **2014**, *140*, 164116.

(113) Holzer, C.; Gui, X.; Harding, M. E.; Kresse, G.; Helgaker, T.; Klopper, W. Bethe-Salpeter Correlation Energies of Atoms and Molecules. *J. Chem. Phys.* **2018**, *149*, 144106.

(114) Li, J.; Duchemin, I.; Blase, X.; Olevano, V. Ground-state correlation energy of beryllium dimer by the Bethe-Salpeter equation. *SciPost Phys.* **2020**, *8*, 20.

(115) Loos, P.-F.; Scemama, A.; Duchemin, I.; Jacquemin, D.; Blase, X. Pros and Cons of the Bethe-Salpeter Formalism for Ground-State Energies. *J. Phys. Chem. Lett.* **2020**, *11*, 3536.

(116) Angyan, J. G.; Liu, R.-F.; Toulouse, J.; Jansen, G. Correlation Energy Expressions from the Adiabatic-Connection Fluctuation Dissipation Theorem Approach. *J. Chem. Theory Comput.* **2011**, *7*, 3116−3130.

(117) Furche, F.; Van Voorhis, T. Fluctuation-Dissipation Theorem Density-Functional Theory. *J. Chem. Phys.* **2005**, *122*, 164106.

(118) Caruso, F.; Rohr, D. R.; Hellgren, M.; Ren, X.; Rinke, P.; Rubio, A.; Scheffler, M. Bond Breaking and Bond Formation: How Electron Correlation Is Captured in Many-Body Perturbation Theory and Density-Functional Theory. *Phys. Rev. Lett.* **2013**, *110*, 146403.

(119) Colonna, N.; Hellgren, M.; de Gironcoli, S. Correlation Energy Within Exact-Exchange Adiabatic Connection Fluctuation-Dissipation Theory: Systematic Development and Simple Approximations. *Phys. Rev. B: Condens. Matter Mater. Phys.* **2014**, *90*, 125150.

(120) Hellgren, M.; Caruso, F.; Rohr, D. R.; Ren, X.; Rubio, A.; Scheffler, M.; Rinke, P. Static Correlation and Electron Localization in Molecular Dimers from the Self-Consistent RPA and G W Approximation. *Phys. Rev. B: Condens. Matter Mater. Phys.* **2015**, *91*, 165110.

(121) Maggio, E.; Kresse, G. Correlation Energy for the Homogeneous Electron Gas: Exact Bethe-Salpeter Solution and an Approximate Evaluation. *Phys. Rev. B: Condens. Matter Mater. Phys.* **2016**, *93*, 235113.

(122) van Setten, M. J.; Caruso, F.; Sharifzadeh, S.; Ren, X.; Scheffler, M.; Liu, F.; Lischner, J.; Lin, L.; Deslippe, J. R.; Louie, S. G.; et al. 100: Benchmarking G_0W_0 for Molecular Systems. *J. Chem. Theory Comput.* **2015**, *11*, 5665−5687.

(123) Maggio, E.; Liu, P.; van Setten, M. J.; Kresse, G. GW 100: A Plane Wave Perspective for Small Molecules. *J. Chem. Theory Comput.* **2017**, *13*, 635−648.

(124) Loos, P. F.; Romaniello, P.; Berger, J. A. Green Functions and Self-Consistency: Insights From the Spherium Model. *J. Chem. Theory Comput.* **2018**, *14*, 3071−3082.

(125) Duchemin, I.; Blase, X. Robust Analytic-Continuation Approach to Many-Body GW Calculations. *J. Chem. Theory Comput.* **2020**, *16*, 1742−1756.

(126) Olivucci, M. *Computational Photochemistry*; Elsevier Science: Amsterdam, 2010.

(127) Navizet, I.; Liu, Y.-J.; Ferre, N.; Roca-Sanjuán, D.; Lindh, R. The Chemistry of Bioluminescence: An Analysis of Chemical Functionalities. *ChemPhysChem* **2011**, *12*, 3064−3076.

(128) Loos, P. F.; Scemama, A.; Jacquemin, D. The Quest for Highly-Accurate Excitation Energies: a Computational Perspective. *J. Phys. Chem. Lett.* **2020**, *11*, 2374.

(129) Roos, B. O.; Andersson, K.; Fulscher, M. P.; Malmqvist, P.-A.; Serrano-Andrés, L. In *Multiconfigurational Perturbation Theory: Applications In Electronic Spectroscopy*; Prigogine, I., Rice, S. A., Eds.; Adv. Chem. Phys.; Wiley: New York, 1996; Vol. *XCIII*, pp 219−331.

(130) Furche, F.; Ahlrichs, R. Adiabatic Time-Dependent Density Functional Methods for Excited State Properties. *J. Chem. Phys.* **2002**, *117*, 7433.

(131) Lazzeri, M.; Attaccalite, C.; Wirtz, L.; Mauri, F. Impact of the Electron-Electron Correlation on Phonon Dispersion: Failure of LDA and GGA DFT Functionals in Graphene and Graphite. *Phys. Rev. B: Condens. Matter Mater. Phys.* **2008**, *78*, 081406.

(132) Faber, C.; Janssen, J. L.; Côté, M.; Runge, E.; Blase, X. Electron-Phonon Coupling in the C_{60} Fullerene within the Many-body *GW* Approach. *Phys. Rev. B: Condens. Matter Mater. Phys.* **2011**, *84*, 155104.

(133) Yin, Z. P.; Kutepov, A.; Kotliar, G. Correlation-Enhanced Electron-Phonon Coupling: Applications of *GW* and Screened Hybrid Functional to Bismuthates, Chloronitrides, and Other High-T_c Superconductors. *Phys. Rev. X* **2013**, *3*, 021011.

(134) Monserrat, B. Correlation Effects on Electron-Phonon Coupling in Semiconductors: Many-Body Theory Along Thermal Lines. *Phys. Rev. B: Condens. Matter Mater. Phys.* **2016**, *93*, 100301.

(135) Li, Z.; Antonius, G.; Wu, M.; da Jornada, F. H.; Louie, S. G. Electron-Phonon Coupling from Ab Initio Linear-Response Theory within the *GW* Method: Correlation-Enhanced Interactions and Superconductivity in $Ba_{1-x}K_xBiO_3$. *Phys. Rev. Lett.* **2019**, *122*, 186402.

(136) Ismail-Beigi, S.; Louie, S. G. Excited-State Forces within a First-Principles Green's Function Formalism. *Phys. Rev. Lett.* **2003**, *90*, 076401.

(137) Rohlfing, M.; Louie, S. G. Electron-hole Excitations and Optical Spectra from First Principles. *Phys. Rev. B: Condens. Matter Mater. Phys.* **2000**, *62*, 4927−4944.

(138) Ma, Y.; Rohlfing, M.; Molteni, C. Excited States of Biological Chromophores Studied Using Many-Body Perturbation Theory: Effects of Resonant-Antiresonant Coupling and Dynamical Screening. *Phys. Rev. B: Condens. Matter Mater. Phys.* **2009**, *80*, 241405.

(139) Ma, Y.; Rohlfing, M.; Molteni, C. Modeling the Excited States of Biological Chromophores within Many-Body Green's Function Theory. *J. Chem. Theory Comput.* **2010**, *6*, 257−265.

(140) Romaniello, P.; Sangalli, D.; Berger, J. A.; Sottile, F.; Molinari, L. G.; Reining, L.; Onida, G. Double Excitations in Finite Systems. *J. Chem. Phys.* **2009**, *130*, 044108.

(141) Sangalli, D.; Romaniello, P.; Onida, G.; Marini, A. Double Excitations in Correlated Systems: A Many−Body Approach. *J. Chem. Phys.* **2011**, *134*, 034115.

(142) Huix-Rotllant, M.; Ipatov, A.; Rubio, A.; Casida, M. E. Assessment of Dressed Time-Dependent Density-Functional Theory for the Low-Lying Valence States of 28 Organic Chromophores. *Chem. Phys.* **2011**, *391*, 120−129.

(143) Zhang, D.; Steinmann, S. N.; Yang, W. Dynamical second-order Bethe-Salpeter equation kernel: A method for electronic excitation beyond the adiabatic approximation. *J. Chem. Phys.* **2013**, *139*, 154109.

(144) Rebolini, E.; Toulouse, J. Range-Separated Time-Dependent Density-Functional Theory with a Frequency-Dependent Second-Order Bethe-Salpeter Correlation Kernel. *J. Chem. Phys.* **2016**, *144*, 094107.

(145) Olevano, V.; Toulouse, J.; Schuck, P. A formally exact one-frequency-only Bethe-Salpeter-like equation. Similarities and differences between GW+BSE and self-consistent RPA. *J. Chem. Phys.* **2019**, *150*, 084112.

(146) Ankudinov, A. L.; Nesvizhskii, A. I.; Rehr, J. J. Dynamic Screening Effects in X-Ray Absorption Spectra. *Phys. Rev. B: Condens. Matter Mater. Phys.* **2003**, *67*, 115120.

(147) Baumeier, B.; Andrienko, D.; Ma, Y.; Rohlfing, M. Excited States of Dicyanovinyl-Substituted Oligothiophenes from Many-Body Green's Functions Theory. *J. Chem. Theory Comput.* **2012**, *8*, 997−1002.